

Time domain characterization of micrometeorological data based on a two sample variance

Peter Werle*

Karlsruhe Institute of Technology KIT, Institute of Meteorology and Climate Research IMK-IFU, Kreuzackbahnstrasse 19, 82467 Garmisch-Partenkirchen, Germany

ARTICLE INFO

Article history:

Received 16 November 2009

Accepted 21 December 2009

Keywords:

Turbulent transport

Eddy correlation

Stationarity

Variance

Greenhouse gases

Tunable diode laser

ABSTRACT

In ecosystem research laser based gas monitors are increasingly used to measure fluxes of methane, nitrous oxide and even stable carbon isotopes. As these complex measurement devices under field conditions cannot be considered as absolutely stable, drift characterization is an issue to distinguish between atmospheric data and sensor drift. In this paper the concept of the two sample variance is utilized in analogy to previous stability investigations to characterize the stationarity of spectroscopic and micrometeorological data in the time domain. The main results of the study are practical guidelines how to use the method for eddy-covariance determination of ecosystem exchange by laser-optical instruments suffering from signal instability. As an example, the method is applied to assess the high-pass filter time constant for detrending of time series data. The method described here provides information similar to existing characterizations as the ogive analysis, the normalized error variance of the second order moment as well as information about the spectral characteristics of turbulence in the inertial subrange. The method is easy to implement and, therefore, well suited to assist as a useful tool for a routine data quality check for both, new practitioners and experts in the field.

© 2009 Elsevier B.V. All rights reserved.

1. Introduction

Integrated ecosystem-atmosphere process studies provide a better understanding how the interacting physical, chemical and biological processes transport and transform energy and matter through the land-atmosphere interface from the cell level to a global scale. To predict the impact of future changes to air quality, climate and ecosystems, there is a need to understand the details of carbon and nitrogen cycling between the terrestrial and atmospheric systems (iLEAPS, 2005). The eddy-covariance technique directly determines the flux of an atmospheric trace gas through a plane parallel to the surface. Ideally, the meteorological conditions controlling the state of the turbulence should not vary over the course of the measurements. The technique requires simultaneous fast and accurate measurements of both the vertical velocity and the trace species in question (Stull, 1988). Fortunately, the technique for the measurement of the turbulence with the necessary resolution is available. Sonic anemometers can readily yield air motion data with the required resolution. The major limitation in the past was the availability of appropriate chemical sensors with sufficient time resolution and sensitivity. Meanwhile the situation has changed significantly and a series of approaches to measuring fluxes of methane and nitrous oxide between landscapes and the atmosphere

has been reported (Denmead, 2008). Diode laser absorption spectroscopy (Werle, 1998) is increasingly being used in atmospheric research and has proven to be an appropriate chemical species sensor with the time response and sensitivity required for direct eddy-correlation flux measurements. Historically most instruments used for greenhouse gas flux measurements were research type spectrometers modified for field applications (Fan et al., 1992; Verma et al., 1992; Wienhold et al., 1994; Smith et al., 1994; Fowler et al., 1995; Edwards et al., 1994; Zahniser et al., 1995; Hovde et al., 1995; Kormann et al., 2001; Werle and Kormann, 2001). Most of these systems were operated by the system developers themselves or at least in close cooperation. Improvements in the quality of semiconductor lasers together with the development of new laser devices (quantum cascade lasers) finally have led to the development of a new generation of diode laser spectrometers (Werle et al., 2008). Today a growing selection of commercial instrumentation for atmospheric research and trace gas flux measurements is available and increasingly being used by ecosystem researchers for greenhouse gas monitoring (Edwards et al., 2003; Kroon et al., 2007; Pihlatie et al., 2005; Patteya et al., 2006; Eugster et al., 2007; Hendriks et al., 2008) and for studies of carbon isotope fluxes (Bowling et al., 2003; Tuzson et al., 2008; Schaeffer et al., 2008). All these laser-optical gas measurements are based on commercially available laser spectrometers for nitrous oxide, methane and carbon dioxide respectively.

The standard procedure in ecosystem research for computing eddy-covariance fluxes using a trace gas analyzer and a sonic

* Tel.: +49 08821 183170; fax: +49 08821 73573.

E-mail addresses: Peter.Werle@kit.edu, Peter.Werle@ino.it.

anemometer is to decompose a time series of the vertical velocity w and the trace gas mixing ratio c into a mean and a perturbation part as

$$c = \bar{c} + c' \quad \text{and} \quad w = \bar{w} + w' \quad (1)$$

where the overbar denotes block time averaging. The flux, F , can be determined with the direct eddy-correlation method by the calculation of the covariances of two measuring quantities w and c of a time series as

$$\langle F \rangle = \langle w' \cdot c' \rangle \quad (2)$$

where the brackets then denote time averaging over the flux averaging timescale (or record length). The averaging associated with the overbar defines the perturbation timescale and the averaging associated with the brackets defines the flux averaging timescale (Vickers et al., 2009; Lenschow et al., 1994). Obviously the choice of the perturbation timescale sets an upper-limit on the range of scales included in the computed flux. Eddy fluxes are representative for a footprint area at the windward side of the measuring point (Schmid, 2002). To control the data quality, stationarity has to be assured during the averaging interval. For the determination of turbulent fluxes sensor signals are typically recorded for about 30 min (or more), depending on the spectra of turbulence. The method outlined above for the calculation of turbulence characteristics is only valid under stationary conditions. The knowledge about the degree of stationarity is important to classify the quality of the results. Foken and Wichura (1996) have introduced a measure for steady-state conditions within an averaging interval. They compared the covariance determined for the full averaging period with the mean covariance derived from typically 4–8 shorter subensemble time scales within this period. The measurement was considered stationary, when the difference between the two values was less than 30% (Foken et al., 2004). Vickers and Mahrt (1997) applied a regression scheme to time series data as a steady-state test and the ‘between-record standard deviation’ of the flux has been investigated by Mahrt (1998). Another criterion related to averaging is based on the so-called ogive analysis. Oncley et al. (1990) introduced the ogive function as a test to check if all low-frequency parts are included in the turbulent flux measured with the eddy-covariance method. The ogive is the cumulative integral of the co-spectrum $Co_{w,y}$ of the turbulent flux starting with the highest frequencies and ending at the frequency of interest f_0 :

$$og_{w,y}(f_0) = \int_{\infty}^{f_0} Co_{w,y}(f) df \quad (3)$$

where w is the vertical wind component, y a scalar quantity. If the ogive is plotted as a function of f_0 , and approaches an asymptote at some period, it indicates that there is no more flux beyond that period (Foken et al., 2006). If such an asymptote is not approached, this is an indicator that the overall integration time for the determination of the net ecosystem exchange has to be extended, for example, due to coherent structures (Gao et al., 1989).

Trends on the observed time series data are mainly caused by drifts of different devices and by non-stationary micrometeorological conditions itself (Lee et al., 2004). Therefore, instrumental effects must be minimized before starting the flux calculation. Several procedures have been described for detrending time series data prior to Reynolds decomposition. Advantages and disadvantages of frequently used procedures like block averaging or removal of the mean, linear detrending (Gash and Culf, 1996) and recursive digital filters have been discussed in detail (Shuttleworth, 1980; Rannik and Vesala, 1999; Moore, 1986 with the corrections of Horst, 2000). Determination of the high-pass filter time constant is a tricky procedure and Moncrieff et al. (2004) conclude in their paper on

averaging, detrending and filtering of eddy-covariance data that ‘no definitive method can be recommended to distinguish sensor drift from true low-frequency atmospheric signal’. The question whether signal changes refer to a drift of the spectrometer itself or reflect a true change in the trace gas mixing ratio is frequently asked when dealing with laser-optical trace gas sensors. Werle et al. (1993) introduced a stability measure for spectroscopic gas analyzers to investigate the limits of signal averaging. This method meanwhile is widely accepted in the spectroscopic community to characterize system performance of field laser applications in industry and research (Werle and D’Amato, 2008). In this paper the two sample variance is introduced as a tool to characterize micrometeorological data in the time domain. The proposed scheme provides a simple but reliable quality control scheme and recommendations can be given to define a time scale, on which system drifts can be separated from atmospheric signals. Based upon this approach, guidelines are discussed that allow an analysis of micrometeorological time series to choose a time constant that serves the best for signal detrending purposes.

2. Mean square successive differences

Already in 1942 von Neuman et al. mentioned that ‘there are cases, where the standard deviation may be held constant. But the mean varies from one observation to the next. If no correction is made for such a variation of the mean and the standard deviation is computed from the data in the conventional way, then the estimated standard deviation value will tend to be larger than the true population value. When the variation in the mean is gradual, so that a trend (which need not to be linear) is shifting the mean, a rather simple method of minimizing the effect of the trend on dispersion is to estimate standard deviation from differences.’ Therefore von Neumann et al. (1942) proposed a variance based upon mean square successive differences. A strategy based upon this approach to investigate turbulent transport will be illustrated and discussed in the following section.

Suppose a time series of a scalar quantity $y(t)$. Fig. 1 shows such a 30 min time series of concentration measurements (18,000 values with a 10 Hz resolution) as measured with a high frequency modulated diode laser spectrometer (Werle and Kormann, 2001) To analyze such time series data, historically, the standard deviation equation has been used:

$$\sigma_{\text{stddev}}^2 = \langle (y_i - \bar{y})^2 \rangle \quad \bar{y} = \frac{1}{T} \cdot \int_0^T y(t) dt \quad (4)$$

where the brackets denote an infinite time average and \bar{y} is the average concentration over the data set with record length T that is

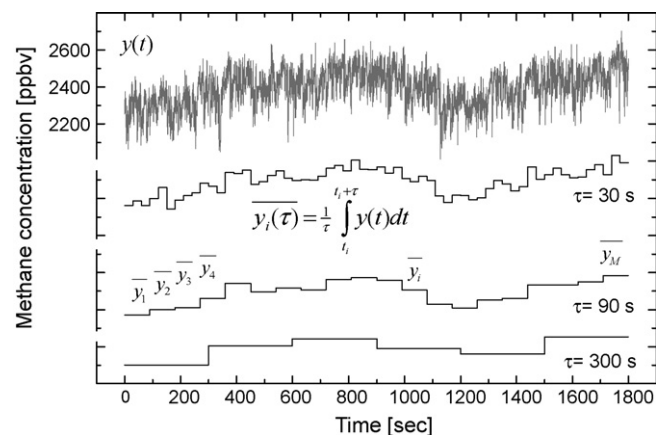


Fig. 1. 30 min time series of methane concentration recorded at 10 Hz together with selected subensemble averages with bin-sizes of 30 s, 90 s and 300 s.

subtracted from each value of y_i before squaring, summing and dividing by the number of values minus one. In 1964 a subcommittee on frequency stability was formed within the Institute of Electrical and Electronic Engineers (IEEE) Standards Committee to prepare an IEEE standard on frequency stability. In 1969, this subcommittee completed a document proposing definitions for measures on frequency and phase stabilities. It has been studied what happens to the standard deviation when the data set may be characterized by power law spectra which are more dispersive than classical white noise frequency fluctuations (Barnes et al., 1971). In other words, if the fluctuations are characterized by flicker noise or any other non-white-noise frequency deviations, what happens to the standard deviation for that data set? One can show that the standard deviation is a function of the number of data points in the set; it is also a function of the dead-time and of the bandwidth of the measurement system. For example, using flicker noise as a model, as the number of data points increases, the standard deviation monotonically increases without limit. The IEEE has adopted a standard measure based upon the two sample standard deviation, also known as the ‘Allan deviation’, which is the square root of the two sample zero dead-time variance $\sigma_y^2(\tau)$ (von Neumann et al., 1942; Allan, 1966; Barnes et al., 1971) and an experimental estimation of this standard measure is

$$\sigma^2(\tau) = \frac{1}{2} \langle (\bar{y}_{k+1} - \bar{y}_k)^2 \rangle \quad \text{with} \quad \bar{y}_k(\tau) = \frac{1}{\tau} \cdot \int_{t_k}^{t_k+\tau} y(t) dt \quad (5)$$

where $t_{k+1} = t_k + \tau$, and k and $k + 1$ are adjacent samples. This equation is easy to implement experimentally: one simply needs to add up the squares of the differences between adjacent averaged $\bar{y}_k(\tau)$ over intervals τ as illustrated in Fig. 1, divide by the number of them and by two, and take the square root. This is the quantity which the IEEE subcommittee has recommended for specification of stability in the time domain denoted by $\sigma_y(\tau)$. This recommended measure of stabilities in frequency generators has gained general acceptance among users of frequency and time standards throughout the world.

In general if the spectral density $S_y(f)$ is known, the two sample variance can be computed as averaging data for a time τ may be thought of as a filtering operation. The transfer function, $H(f)$, of this equivalent filter is the Fourier transform of the impulse response of the filter. The time domain stability according to Barnes et al. (1971) is given by the average value of the sample variance of M averages of $y(t)$ each of duration τ and spaced every T units of time:

$$\langle \sigma^2(M, T, \tau) \rangle = \int_0^\infty S_y(f) \cdot |H(f)|^2 df \quad (6)$$

Differences between τ and T are due to limitations in the data acquisition, which cause a “dead-time” (Werle et al., 1993). $S_y(f)$ is the spectral density of the quantity y (Rutman, 1972) and in the case of the two sample variance:

$$|H(f)|^2 = \frac{2 \sin^4(\pi f \tau)}{(\pi f \tau)^2} \quad (7)$$

and the two sample variance can thus be computed from

$$\langle \sigma^2(\tau) \rangle = 2 \int_0^\infty S_y(f) \cdot \frac{\sin^4(\pi f \tau)}{(\pi f \tau)^2} df \quad (8)$$

For a given power law model $S_y(f) \propto f^\mu$, the time domain measure $\sigma_y^2(\tau) \propto \tau^\alpha$ also follows a power law for integer values as $\alpha = -\mu - 1$. Typical power laws encountered in most systems are the frequency independent white noise ($\mu = 0$) and frequency dependent $1/f^\mu$ noise ($\mu \geq 1$) referred to as $1/f$ -noise, flicker noise and random walk. The latter noise encompasses a noise at very low

frequencies which can be considered as drift. White noise can be reduced by bandwidth reduction, which is equivalent to integration and the two sample variance decreases (proportional to $1/\tau$, $\alpha = -1$) with increasing integration time. The contributions from $1/f$ -noise remain constant for all averaging times. With increasing integration time, the Allan variance shifts into a region, where drifts and discrete frequency interferences dominate and where it again starts to increase (proportional to the measurement time, τ) or may oscillate in the case of periodic interferences. When $\sigma_y^2(\tau)$ is plotted on a double logarithmic scale versus the averaging interval τ one obtains an ‘Allan plot’ as shown in Fig. 2., where, for example, the raw time series data of Fig. 1 lead to a minimum in the two sample variance for an averaging interval of approximately 60 s. The decreasing dashed line shows the theoretically expected τ^{-1} behaviour of a stationary data set dominated by white noise. The Allan plot provides useful time domain information as the minimum in the two sample variance at τ_{opt} can be interpreted as the maximum integration time. This time is a characteristic property for a given instrument or measurement condition, because it represents the time during which we can assume stationary conditions for the data set under investigation (Werle et al., 1993).

3. Trend removal from time series data

Digital filters can be applied in the time domain and in the frequency domain. Time domain filtering is used for smoothing and offset removal, while frequency domain filters are used when the required information is contained in the amplitude, frequency and phase of the component sinusoids. Digital filters can be implemented in two ways, by convolution (also called finite impulse response or FIR) and by recursion (also called infinite impulse response or IIR). Filters carried out by convolution can have far better performance than filters using recursion, but execute much more slowly (Smith, 1997). When convolution (denoted by $*$) is used with linear systems, an input signal, $x(t)$, enters a linear system with an impulse response, $h(t)$, resulting in an output signal $y(t) = h(t) * x(t)$.

$$y(t) = \int_{-\infty}^{+\infty} h(\tau) \cdot x(t - \tau) d\tau \quad \leftrightarrow \quad y[i] = \sum_{j=0}^{M-1} h[j] \cdot x[i - j] \quad (9)$$

where in the discrete representation the index, i , determines which sample in the output signal is being calculated. As j runs through 0 to $M - 1$, each sample in the impulse response, $h[j]$, is multiplied by the proper sample from the input signal, $x[i - j]$. The group of

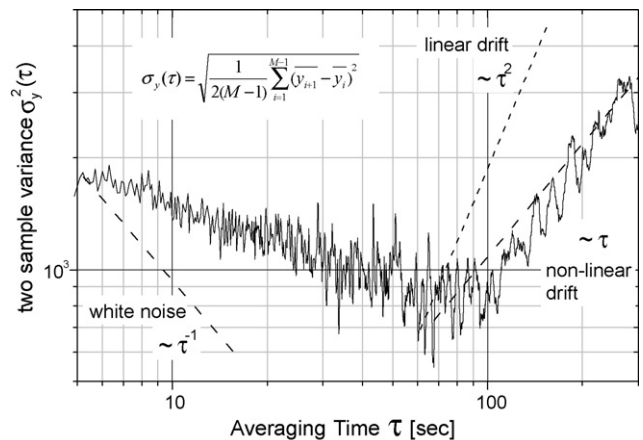


Fig. 2. Plot of the two sample variance as a function of the subensemble averaging time τ . The dashed line following τ^{-1} indicates the expected behaviour for a white noise dominated system.

points from the input signal can be chosen symmetrically around the output point, which requires M to be an odd number. This corresponds to changing the summation from $j = 0$ to $M - 1$, to $j = -(M - 1)/2$ to $(M - 1)/2$. Even if programming of the single sided filter is slightly easier, this produces a relative shift between the input and output signals, which is not desired for the detrending application. The moving average filter is optimal for reducing random white noise while keeping sharpest step response. The low-pass cut-off is very slow and there are still contributions in frequency ranges, where the signal should be completely suppressed, but in the time domain the moving average is an exceptionally good smoothing filter. This filter operates by averaging a number of points from the input signal to produce each point in the output signal. The moving average filter is a convolution using a very simple filter kernel (another name for a filter's impulse response) $h[j] = 1/M$ with a rectangular pulse of a unit area (width τ and height $1/\tau$) and now in symmetric summation notation is

$$y[i] = \sum_{j=-(M-1)/2}^{(M-1)/2} \frac{1}{M} \cdot x[i - j] \quad (10)$$

When the frequency spectrum of the rectangular pulse is not aliased (because the time domain signal is continuous, or because aliasing is ignored), it is of the general form: $\sin(x)/x$, i.e., a sinc function. The frequency response of the moving average (low-pass) filter is mathematically described by the Fourier transform of the rectangular pulse:

$$H_{LP}(f) = \frac{\sin(\pi fM)}{\pi fM} \quad (11)$$

An example of the effect of the moving average filter for selected time constants of 30 s, 90 s, 300 s and 600 s is shown in Fig. 3. The raw data from Fig. 1 are plotted again in Fig. 3a together with low-pass filtered data using varying filtering times, while in Fig. 3b the detrended time series is shown. Trend removal requires a high-pass filter. High-pass filters are designed by starting with a low-pass filter, and then converting it into the desired response. A method for the low-pass to high-pass conversion is spectral inversion. This is performed by flipping the frequency response top-to-bottom, which changes a filter from low-pass to high-pass. The overall output, $y(t)$, then is equal to the output of an all-pass system represented by the a delta function, $\delta(t)$, minus the output of the low-pass system, $h(t)$.

$$y(t) = [\delta(t) - h(t)] * x(t) \quad (12)$$

Such a two step modification to the time domain results in an inverted frequency spectrum. Since the low-frequency components are subtracted from the original signal, only the high frequency components appear in the output and a high-pass filter is formed. In a computer program this can be performed as a two step operation: run the signal through a low-pass filter (here a moving average), and then subtract the filtered signal from the original, but the entire operation can be performed in a single stage by combining the two filter kernels. The filter kernel for the high-pass filter is given by $[\delta(t) - h(t)]$. That is obtained by changing the sign of all the samples, and then adding one to the sample at the centre of symmetry. For this technique to work, the low-frequency components exiting the low-pass filter must have the same phase as the low-frequency components exiting the all-pass system. Otherwise a complete subtraction cannot take place. This places two restrictions on the method: (i) the original filter kernel must have left-right symmetry (i.e., a zero or linear phase), and (ii) the impulse must be added at the centre of symmetry. The result of the detrending procedure is shown in Fig. 3b for the same time constants as in the previous case. It is worth to be noted that the

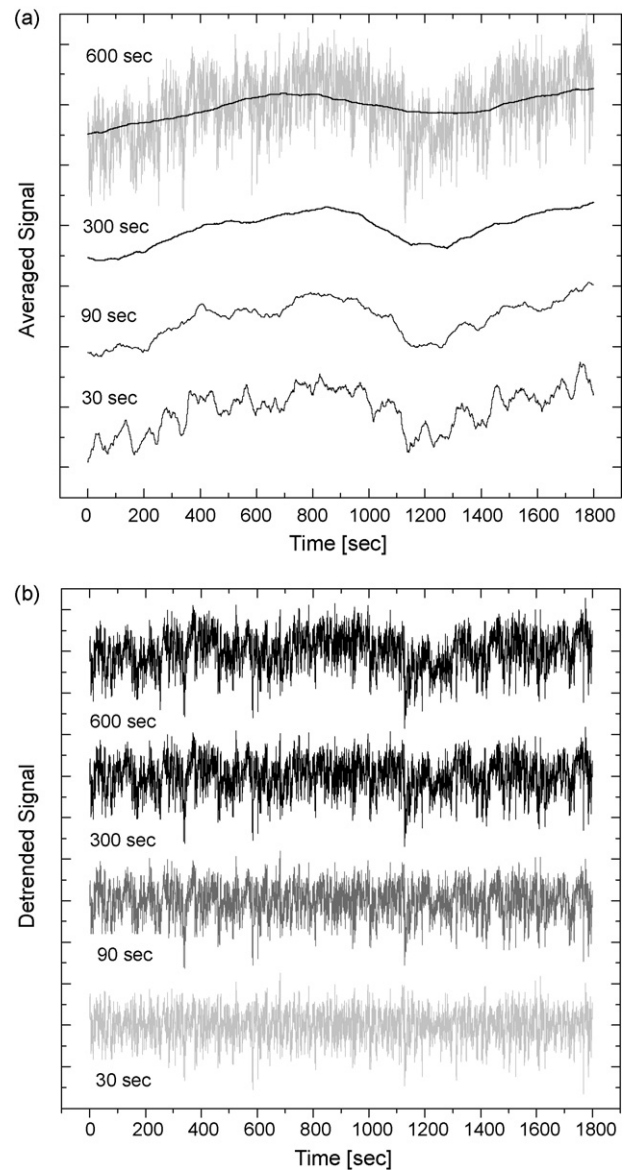


Fig. 3. (a) Smoothing effect of the moving average filter with different time constants and (b) corresponding detrended time series data.

600 s time constant might have been chosen too long as now artefacts are introduced due to smoothing that extends beyond interfering structures in the time series and the limit case of the removal of the mean is approached.

4. Discussion

So far we have seen that detrending can be interpreted in general as high-pass filtering. An open question is still, whether we can estimate a filter time constant for a detrend procedure. Obviously the time constant has to be chosen in accordance with a given stability of the system and measurement signal. Therefore, it is a prerequisite to provide an accurate system characterization prior to a measurement at a field site. Even if the concept described here is valid in general for all scalar parameters involved in eddy-covariance measurements, the discussion will focus on fast trace gas concentration measurements by laser-optical sensors. There can occur complex interferences that have to be understood in order to separate what is system related from what can be attributed to the ambient signal. Laser light that is tuned to a characteristic “fingerprint” absorption of a selected trace gas under

investigation has a very narrow spectral width. Such a monochromatic beam in the infrared spectral region has a wavelength of a few microns and is then tuned over a spectral feature to selectively measure a characteristic absorption signal (Werle, 1998). Most techniques and instruments require a reference to a stable background signal. In practice, this is available only in a limited sense (Werle et al., 1993). Even in the absence of a trace gas absorption (e.g. when the analyzers sample cell is flushed with zero air) fluctuations and drifts occur. A typical mechanism that causes such a drift is the étalon or fringe effect, which is caused by the resonant interaction of the monochromatic laser light with structures in the optical system. In principle, they could be filtered out—if they were stable. Depending on the interacting optical scales they can form complex time dependent structures and are superimposed to the desired spectroscopic signal, which in turn can become cumbersome if close to the detection limit everything is buried in noise.

The key issue to measure long wavelength atmospheric contributions is the separation of (i) instrumental “drift” effects and (ii) atmospheric contributions. Therefore, it is strongly recommended to characterize any spectrometer prior to field measurements in the lab and again frequently and preferably automated on-site. The most straight forward and recommended method is to generate a ‘horizontal line’. This means that the analyzer should be flushed with calibration gas at or near ambient concentrations and then the concentration signal versus time should be recorded (Werle et al., 2004). Well maintained calibration sources for greenhouse gases should not vary over a typical period of observation. The first step is to record time series concentration data from a stable calibration gas source without letting ambient air entering the measurement cell. In this case no atmospheric contribution to the signal is present and also no gas induced signal variations will occur. An ideal system would provide a record of constant calibration values over the measurement time. In a real world system all changes that can now be observed in the time series data record are due to instrumental drift. Analyzing such a time series in terms of the two sample variance, provides an estimate for the stability timescale, τ_{opt} , of the instrument and the necessary information to determine calibration and background measurement cycles. If such a maximum integration time has been determined, the ambient spectra as well as the corresponding background/calibration spectra must be measured within this time interval τ_{opt} . Longer wavelengths of atmospheric phenomena cannot be studied with formal spectral analysis in the case of sensors with this drift characteristic, but as discussed later in this paper, eddy covariance that includes the longer-wavelength contributions can still be performed. τ_{opt} can be seen as a stability time constant for the system in the sense that any data recorded at a time t_0 still describe the state of the system correct at $t_0 + \tau_{\text{opt}}$. Typically spectroscopic instruments for eddy correlation provide concentration data at 10 Hz. The laser is scanned at a high repetition rate over a spectral absorption line (of methane, for example) and the detector signal is averaged for 100 ms to increase the signal-to-noise-ratio. Each of these averaged scans again contains an absorption signal plus a spectral background signal, which has been explained earlier in the manuscript when the étalon effect was discussed. Therefore, a background signal (=air without the target gas, here methane) has to be recorded at t_0 and must be stored in the computer. This background signal has to be subtracted from all subsequent averaged scans following t_0 and each 10 Hz raw concentration is therefore corrected immediately. The stability time constant τ_{opt} defines the interval $[t_0, t_0 + \tau_{\text{opt}}]$ within which this subtraction is allowed. For times $t > t_0 + \tau_{\text{opt}}$ a relationship between the signal from the sample and the previous background recorded at t_0 is lost and the subtraction would introduce a drift error (Werle et al., 2004). Therefore within the interval $[t_0, t_0 + \tau_{\text{opt}}]$ a recalibration is

necessary in the sense that the background has to be updated for the next interval of length τ_{opt} . For comparable signal-to-noise-ratio the background recording requires also 100 ms plus some time for the gas exchange and settling (about 10–20 s, but could be even faster). As the instrumental drift is now monitored in the time dependent background record, this procedure assures continuous drift correction on a 10 Hz scale, provided τ_{opt} has been chosen properly. After the system has been characterized and measurement cycles have been setup properly it can be used now for ambient measurements. With this approach, fluctuations on a shorter time scale than τ_{opt} can be clearly attributed to changes in the atmospheric sample and in order to measure long wavelength atmospheric contributions for longer time scales one can simply cascade several shorter block averages separated by the recalibration as described above. This procedure significantly reduces drift effects and is the only way to ensure that drift does not degrade the system performance. In principle, the observed drift should be eliminated, but, practically, residual drifts will occur, which are of importance for ultrasensitive measurements requiring very long averaging times. Therefore, the resulting data can be again analyzed in terms of the two sample variance to validate the procedure. Such an “advanced stage” Allan plot gives an estimate for the final system stability time scale, which can be achieved and using this procedure stability intervals of hours required for very high precision concentration measurements (e.g. HO₂ radicals) can be obtained (Werle, 1996).

Instruments characterized by the method described above have been used during a field campaign on methane fluxes, where laser based eddy-correlation systems have been compared with automated closed chambers and a positive correlation between the measured methane flux, the friction velocity, the horizontal wind and the temperature has been found (Werle and Kormann, 2001). A significant difference between the closed chambers and the EC measurement has been observed, but then at higher wind speed the flux measured in the open approached the chamber data again. An attempt to explain this differences was to attribute the difference to the artificial turbulence in the closed chambers due to the stirring fan inside. This finding meanwhile has been confirmed by Denmead (2008). The time series data shown in Fig. 1 have been recorded during this field campaign at a height of 3.2 m and the data have been analyzed using different time constants for the previously described moving average detrend filter ranging from 30 s to 600 s. In Fig. 4a and b the 30 min averaged flux is plotted as a function of the detrend averaging time constant applied to the time series data as shown in Fig. 3. The calculation of the flux has been performed twice for all detrend time constants: While Fig. 4a shows the results for a 6 s time shift between the fluctuations of the vertical wind w' and the concentrations c' , the results plotted in Fig. 4b have been obtained without accounting for a time lag. Fig. 4c shows the dependence of the calculated cross-covariance function on the time lag between w' and c' for a fixed integration time of 300 s. The dashed lines illustrate how the flux increases, when the time lag is increased from “zero lag” (corresponding to Fig. 4b) to the “peak lag” at 6 s time lag (corresponding to Fig. 4a). A significant variation can be observed for short integration intervals as well as a tendency for a lower flux at long integration times. Accounting for the time delay arising from the flow tube is a prerequisite to obtain reliable results and it can be seen in Fig. 4c that the flux varies from –1 to +9 ppb m/s and around the peak a change of the flux of 4.5 ppb m/s of time lag is calculated. Therefore, a change of the time lag of 1 s transforms into 50% error in the reported peak flux. The very steep cross-covariance function can be attributed to the relatively high wind speed condition of 2.3 m/s. Accounting for time lags is especially critical with laser based analyzers requiring long sampling tubes and when unstabilized sampling systems are used. The application of a fixed time constant should therefore be avoided.

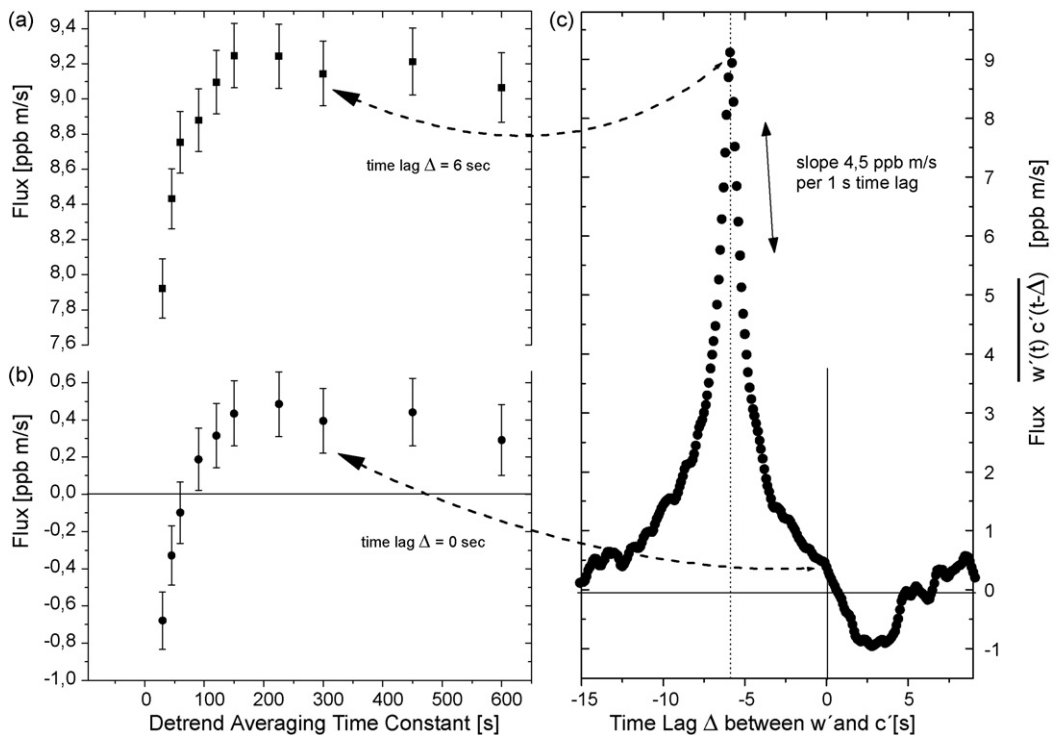


Fig. 4. (a) Calculated fluxes for different time constants of the detrend moving average filter. (b) For comparison the same analysis is shown on the same vertical scale without accounting for a time lag. (c) The covariance for a fixed detrend time constant of 300 s is plotted as a function of the time lag between the fluctuations of the vertical wind and the trace gas concentration. The dashed lines connect the corresponding fluxes in the graph.

The Allan plot in Fig. 2 has been derived from the raw time series of atmospheric trace gas concentrations and indicates a minimum at about 60 s. In the previous section it has been shown that from the slope at longer averaging times we can conclude that there is a non-linear drift. Both fringes in the sense described above and atmospheric turbulent structures may have such a non-linear characteristic and such a (somehow periodic) structure could be observed in the raw time series. The Allan plot ‘detects’ a drift influence for integration times around 60 s. As a next step the high-pass filtered data as shown in Fig. 3b have been analyzed for the range of time constants listed in Fig. 4 in terms of the two sample variance as discussed above. To avoid confusion, only 3 selected curves are displayed in the overview Allan plot in Fig. 5. For averaging intervals below 1 s atmospheric turbulence is resolved for an instrument with a 10 Hz resolution and appears as a drift. This range corresponds to the inertial subrange (Kaimal et al., 1972). As soon as $1/f$ -type noise dominates for longer integration times, the two sample variance remains at a constant level for increasing integration time ($f^{-1} \leftrightarrow \tau^0$). For sufficiently long integration time fast fluctuations will contribute less and less to the variance and white noise ($f^0 \leftrightarrow \tau^{-1}$) as the dominating noise source now will be averaged leading to a decreasing Allan variance (Slope = -1) up to a point where drift effects again start to influence the measurement, i.e., the stationarity of the measurement is no longer valid. The upper right curve shows the drift dominated behaviour of the raw data without any detrending. The middle curve corresponds to 300 s moving average filter for detrending and the lower curve belongs to the 30 s time constant. With respect to the discussion about the Allan plot we can relate the slope in the two sample variance of -2 to a frequency dependence ($f^1 \leftrightarrow \tau^{-2}$) proportional to f , which obviously can be attributed to the low-frequency roll-off of the high-pass filter. It has to be mentioned that for longer averaging times the variance of the two sample variance becomes larger and larger, as it is calculated from less and less samples. While there are 9000 samples used to calculate the two sample variance for 0.1 s

integration time this number reduces to only 9 samples for 100 s. Therefore, any structures observed for long integration times should not be overemphasized. However, from the Allan plot we can see that optimum detrending can be expected for time constants between 100 s and 450 s. The larger value of 600 s leads to artefacts as it can be seen in the upper trace of Fig. 3, where the low-pass filtered signal is shown together with the raw data in grey.

Depending on the measurement conditions, which determine the frequency behaviour of atmospheric turbulence, high-pass filtering leads to low-frequency under-estimation of flux. The laser

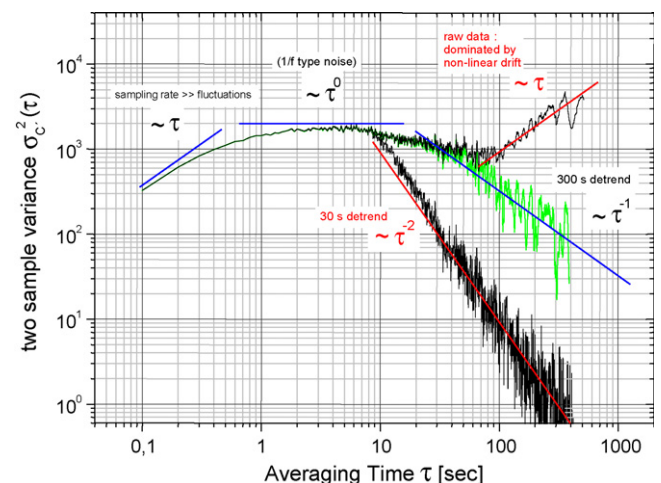


Fig. 5. Two sample variance characterization of a trace gas concentration time series in the time domain. For averaging intervals below 1 s atmospheric turbulence is well resolved and appears as a drift, while in the range between 1 s to 10 s a kind of ‘flicker noise’ dominates. The upper right part shows the drift dominated raw data. The middle curve can be considered as ideal and corresponds to the application of a 300 s moving average filter for detrending. The lower curve belongs to the 30 s time constant.

spectrometer used for the analysis presented here was not dominated by drift up to about 300 s (Werle and Kormann, 2001). This instrument stability has been derived from a two sample variance analysis based on time series data recorded at ambient level calibration gas concentrations under field conditions following the ‘horizontal line approach’ described in the previous section. For longer time intervals the stability of the instrument is not assured and instrument drifts and atmospheric effects are superimposed and therefore, as discussed earlier, it is necessary to complete a “recalibration” of the system within the time interval τ_{opt} of 300 s by applying an appropriate measurement cycle (Werle, 1996). The overall integration time scale for the turbulent fluxes was chosen to be approximately 30 min, interrupted by a short calibration of the laser spectrometer that lasted for typically 20 s (Werle and Kormann, 2001). This procedure ensured that during the whole measurement interval the system stability was

maintained and all measured variations can be attributed to atmospheric signals. By investigating, for example, 300 s intervals, one obtains 6 data points within the observation period of 30 min to resolve low-frequency structures. Although this data segmenting now prevents a conventional Fourier spectrum from being taken of the discontinuous 30 min data set, eddy-covariance calculations can still be performed (Bosveld and Beljaars, 2001). The concept is that so long as the sensors are sensitive to the frequencies in question, sparse sampling in time (not every data point) still gives an accurate (but not as precise as using every data point) calculation of eddy covariance. Spectral correction for high frequency sensor loss can be performed either with the original dataset or the 6 dataset segments, because only the higher frequency response is the objective of such correction, and the lower frequency drift issues would not substantially affect the higher frequency portion of the spectrum.

So far only time series concentration data have been shown. To complete the picture, Fig. 6a shows the frequency domain spectrum of the vertical wind according to Kaimal et al. (1972) together with the time domain Allan plot of the vertical wind after detrended with the same time constant as the concentration data. Finally, in the lower part the flux calculated from detrended and time lag corrected data is shown. A minimum in the Allan plot can be identified for an integration time of 300 s. This reflects the time constant, which has been chosen for the detrend procedure. As a consequence, the data can be chosen in subsamples of 300 s, which in turn leads to 6 sequential discontinuous segments, separated by the recalibration intervals. These segments are then concatenated (‘glued’) together, and the standard eddy-covariance method is then applied to this entire modified dataset. Note that the discontinuities preclude formal spectral analysis of this modified dataset, and also that the 6 segments should not be individually used to calculate 6 separate eddy covariances, later to be averaged. This latter method would lose the lower frequency atmospheric contributions, because the variable means would be recalculated for each of these shorter segments. The resulting number of data points is now less than 18,000 for 10 Hz data in a 30 min record, by the amount of data points in the 5 intervals of ‘on-the fly’ recalibrations (which depend on the interval length needed for reliable recalibration, including pressure/flow equilibration associated with the valve manifold system; in the example here of approximately 20 s recalibration intervals, 1000 points would be lost, leaving 17,000 points used, implying only a small effect on eddy-covariance precision).

5. Summary and conclusions

Since chemical sensors with the time response and sensitivity required for direct eddy-correlation flux measurements are commercially available, such laser-optical systems based on semiconductor diodes are increasingly being used by researchers to determine net ecosystem exchange and turbulent exchange of greenhouse gases between the biosphere and the atmosphere. The focus of this contribution was set on filtering and detrending of concentration time series, but the findings reported here are not limited to this case and can be generally applied, whenever stationarity is investigated.

The two sample variance provides in a single plot similar information as the normalized error variance of the second order moment by Lenschow et al. (1994), the ogive analysis introduced by Oncley et al. (1990), the spectral characteristics of turbulence described by Kaimal et al. (1972) and the stability criteria by Foken and Wichura (1996). Therefore, this analysis can be used to characterize instrumentation in the laboratory prior to field measurements, check instrument performance at field site and during campaigns, determine the detrend time constant and finally

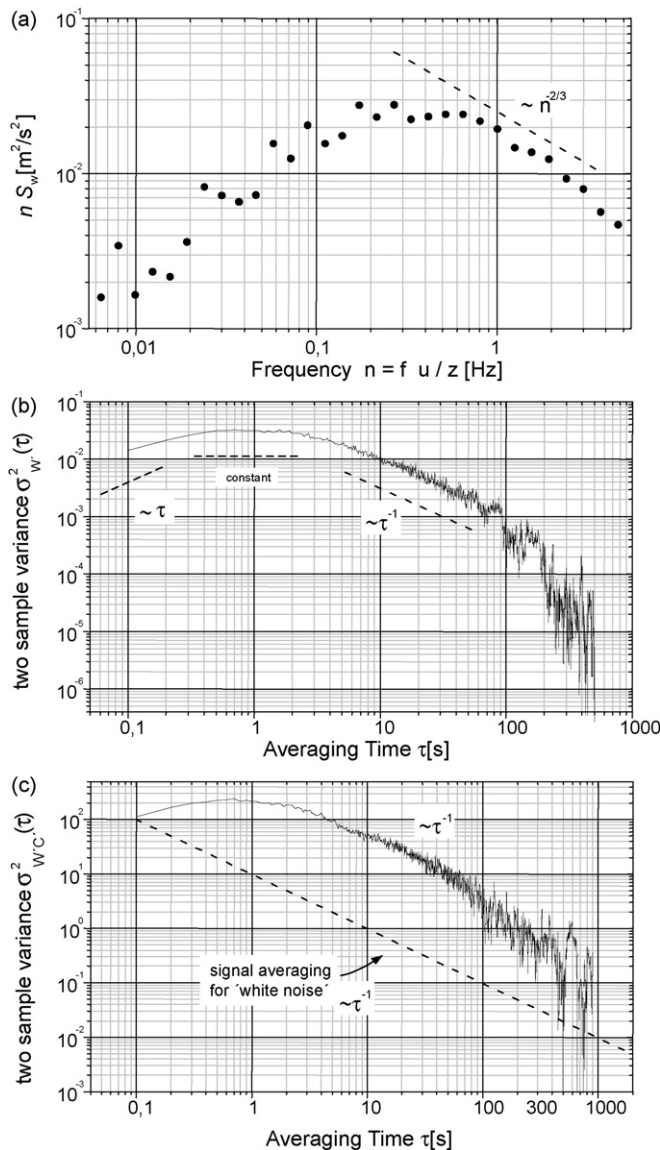


Fig. 6. (a) Frequency domain characterization of the vertical wind fluctuations with the expected behaviour proportional to the normalized frequency $n^{-2/3}$ according to Kaimal et al. (1972). (b) Corresponding two sample variance in the time domain, where the dashed lines show the expected characteristics of a ‘good’ data set. (c) Allan plot for the calculated covariance. A weak minimum can be identified for 300 s integration time, which reflects the filter time constant chosen for the detrend data processing. The dashed line shows the expected behaviour for a ‘white noise’ source in absence of any turbulence, drift or flicker noise contributions.

it can define a roadmap for a data quality assurance. For non-meteorologists and non-spectroscopists it is a useful tool as the algorithm is easy to implement experimentally. When applied for the characterization of micrometeorological data, a 'good' Allan plot should start with an increasing two sample variance, indicating that turbulence is resolved. After passing through a horizontal plateau, the two sample variance should decrease with a slope of -1 on a log-log scale and as long as it remains there, the two sample variance can be used to predict the error of the averaged scalar as a function of the integration time (Werle et al., 1993). A prerequisite for the data analysis is a periodic 'on-the-fly' instrument recalibration with standard gases, without the ambient air sample under investigation, necessitating some form of manifold/valve system. The resulting segmented dataset, after concatenation, can be used for eddy covariance without significant loss of the contributions from potential longer-wavelength atmospheric phenomena, and without significant loss in eddy-covariance precision. This is of importance to distinguish atmospheric signals and coherent structures (Gao et al., 1989) from instrumental effects, especially when they are periodic as the optical fringe effects discussed above. The generation of a horizontal line approach based on a time series recording of a calibration gas provided on-site with a concentration close to the expected ambient concentration levels and an experimentally optimized measurement cycle, give the required confidence about data quality and system stability and can be recommended to distinguish sensor drift from true low-frequency atmospheric signal. If the optimum integration time has been determined for an instrument, it may be necessary to check its value for time to time, especially under field operating conditions, where parameters could change and degrade the system performance. An automated spectrometer can run the stability tests under computer control by analyzing a time series of low level calibration data and adopt automatically the new measurement cycle. Therefore, the approach described in this paper may assist to assure data quality in the emerging field of ecosystem research using modern laser-optical gas analyzers.

Acknowledgement

The valuable comments of Kyaw Tha Paw U are gratefully acknowledged.

References

- Allan, D.W., 1966. Statistics of atomic frequency standards. *Proc. IEEE* 54, 221–230.
- Barnes, J.A., Chi, A.R., Cutler, L.S., Healey, D.J., Leeson, D.B., McGunigal, T.E., Mullen, J.A., Smith, W.L., Sydnor, R.L., Vessot, R.F.C., Winkler, G.M., 1971. Characterization of frequency stability. *IEEE Trans. Instrum. Meas.* IM-20, 105–120.
- Bosveld, F.C., Beljaars, A.C.M., 2001. The impact of sampling rate on eddy-covariance flux estimates. *Agric. For. Meteorol.* 109, 39–45.
- Bowling, D.R., Sargent, S.D., Tanner, B.D., Ehleringer, J.R., 2003. Tunable diode laser absorption spectroscopy for stable isotope studies of ecosystem-atmosphere CO₂ exchange. *Agric. For. Meteorol.* 118, 1–19.
- Denmead, O.T., 2008. Approaches to measuring fluxes of methane and nitrous oxide between landscapes and the atmosphere. *Plant Soil* 309, 5–24.
- Edwards, G.C., Neumann, H.H., den Hartog, G., Thurtell, G.W., Kidd, G., 1994. Eddy correlation measurements of methane fluxes using a tunable diode laser at the Kinosho Lake tower site during the northern wetlands study (NOWES). *J. Geophys. Res.* 99, 1511–1517.
- Edwards, G.C., Thurtell, G.W., Kidd, G.E., Dias, G.M., Wagner-Riddle, C., 2003. A diode laser based gas monitor suitable for measurement of trace gas exchange using micrometeorological techniques. *Agric. For. Meteorol.* 115, 71–89.
- Eugster, W., Zeyer, K., Zeeman, M., Michna, P., Zingg, A., Buchmann, N., Emmenegger, L., 2007. Methodical study of nitrous oxide eddy covariance measurements using quantum cascade laser spectrometry over a Swiss forest. *Biogeosciences* 4, 927–939.
- Fan, S.M., Wofsy, S.C., Bakwin, P.S., Jacob, D.L., Anderson, S.M., Keibabian, P.L., McManus, J.B., Kolb, C.E., Fitzjerald, D.R., 1992. Micrometeorological measurements of CH₄ and CO₂ exchange between the atmosphere and the arctic tundra. *J. Geophys. Res.* 97, 16627–16643.
- Foken, Th., Wichura, B., 1996. Tools for quality assessment of surface-based flux measurements. *Agric. For. Meteorol.* 78, 83–105.
- Foken, Th., Göckede, M., Mauder, M., Mahrt, L., Amiro, B.D., Munger, J.W., 2004. Post-field data quality control. In: Lee, X., Massman, W.J., Law, B. (Eds.), *Handbook of Micrometeorology: A Guide for Surface Flux Measurement and Analysis*. Kluwer, Dordrecht, pp. 181–208.
- Foken, Th., Wimmer, F., Mauder, M., Thomas, C., Liebethal, C., 2006. Some aspects of the energy balance closure problem. *Atmos. Chem. Phys. Discuss.* 6, 3381–3402.
- Fowler, D., Hargreaves, K.J., Skiba, U., Milne, R., Zahniser, M.S., Moncrieff, J.B., Beverland, I.J., Gallagher, M.W., 1995. Measurements of CH₄ and N₂O fluxes at the landscape scale using micrometeorological methods. *Philos. Trans. R. Soc. Lond. Ser. A* 351, 339–356.
- Gao, W., Shaw, R.H., Paw, U.K.T., 1989. Observation of organized structure in turbulent flow within and above forest canopy. *Boundary-Layer Meteorol.* 47, 349–377.
- Gash, J.H.C., Culf, A.D., 1996. Applying a linear detrend to eddy correlation data in real time. *Boundary-Layer Meteorol.* 79, 301–306.
- Hendriks, D.M.D., Dolman, A.J., van der Molen, M.K., van Huissteden, J., 2008. A compact and stable eddy covariance set-up for methane measurements using off-axis integrated cavity output spectroscopy. *Atmos. Chem. Phys.* 8, 431–443.
- Horst, T.W., 2000. On frequency response corrections for eddy covariance measurements. *Boundary-Layer Meteorol.* 94, 517–520.
- Hovde, D.C., Meyers, T.P., Stanton, A.C., Matt, D.R., 1995. Methane emissions from a landfill measured by eddy correlation using a fast response diode laser sensor. *J. Atmos. Chem.* 20, 141–162.
- iLEAPS, 2005. Science Plan and Implementation Strategy. IGBP Report 54. IGBP Secretariat, Stockholm, 52 pp.
- Kaimal, J.C., Wyngaard, J.C., Izumi, Y., Cote, O.R., 1972. Spectral characteristics of surface-layer turbulence. *Q. J. R. Meteorol. Soc.* 98, 563–589.
- Kroon, P.S., Hensen, A., Jonker, H.J.J., Zahniser, M.S., van't Veen, W.H., Vermeulen, A.T., 2007. Suitability of quantum cascade laser spectroscopy for CH₄ and N₂O eddy covariance flux measurements. *Biogeosciences* 4, 715–728.
- Kormann, R., Müller, H., Werle, P., 2001. Eddy flux measurements of methane over the fen Murauer Moos, 11°11'E, 47°39'N, using a fast tunable diode laser spectrometer. *Atmos. Environ.* 35, 2533–2544.
- Lee, X., Massman, W., Law, B. (Eds.), 2004. *Handbook of Micrometeorology—A Guide for Surface Flux Measurement and Analysis Series*, vol. 29. Atmospheric and Oceanographic Sciences Library.
- Lenschow, D.H., Mann, J., Kristensen, L., 1994. How long is long enough when measuring fluxes and other turbulence statistics? *J. Atmos. Ocean. Technol.* 18, 661–673.
- Mahrt, L., 1998. Flux sampling errors for aircraft and towers. *J. Atmos. Oceanic Technol.* 15, 416–429.
- Moncrieff, J., Clement, R., Finnigan, J., Meyers, T., 2004. Averaging, detrending, and filtering of eddy covariance time series. In: Lee, X., Massman, W.J., Law, B. (Eds.), *Handbook of Micrometeorology: A Guide for Surface Flux Measurement and Analysis*. Kluwer, Dordrecht, pp. 7–31.
- Moore, C.J., 1986. Frequency response corrections for eddy correlation systems. *Boundary-Layer Meteorol.* 37, 17–35.
- Oncley, S.P., Businger, J.A., Itsweire, E.C., Friehe, C.A., LaRue, J.C., Chang, S.S., 1990. Surface layer profiles and turbulence measurements over uniform land under near-neutral conditions. 9th Symp. on Boundary Layer and Turbulence, Roskilde, Denmark. *Am. Meteorol. Soc.* 237–240.
- Patteya, E., Strachan, I.B., Desjardins, R.L., Edwards, G.C., Dowa, D., MacPherson, J.I., 2006. Application of a tunable diode laser to the measurement of CH₄ and N₂O fluxes from field to landscape scale using several micrometeorological techniques. *Agric. For. Meteorol.* 136, 222–236.
- Pihlatie, M., Rinne, J., Ambus, P., Pilegaard, K., Dorsey, J.R., Rannik, Ü., Markkanen, T., Launiainen, S., Vesala, T., 2005. Nitrous oxide emissions from a beech forest floor measured by eddy covariance and soil enclosure techniques. *Biogeosciences* 2, 377–387.
- Rannik, Ü., Vesala, T., 1999. Autoregressive filtering versus linear detrending in estimation of fluxes by the eddy covariance method. *Boundary-Layer Meteorol.* 91, 259–280.
- Rutman, J., 1972. Comment on 'Characterization of frequency stability'. *IEEE Trans. Instrum. Meas.* IM-21, 85.
- Schaeffer, S.M., Miller, J.B., Vaughn, B.H., White, J.W.C., Bowling, D.R., 2008. Long-term field performance of a tunable diode laser absorption spectrometer for analysis of carbon isotopes of CO₂ in forest air. *Atmos. Chem. Phys.* 8, 5263–5277.
- Schmid, H.P., 2002. Footprint modeling for vegetation atmosphere exchange studies: a review and perspective. *Agric. For. Meteorol.* 113, 159–184.
- Shuttleworth, W.J., 1980. Corrections for the effect of background concentration change and sensor drift in real-time eddy correlation systems. *Boundary-Layer Meteorol.* 42, 167–180.
- Smith, K.A., Clayton, H., Arah, J.R.M., Christensen, S., Ambus, P., Fowler, D., Hargreaves, K.J., Skiba, U., Harris, G.W., Wienhold, F.G., Klemedtsson, L., Galle, B., 1994. Micrometeorological and chamber methods for measurement of nitrous oxide fluxes between soils and the atmosphere: overview and conclusion. *J. Geophys. Res.* 99, 16541–16548.
- Smith, S.W., 1997. *The Scientist and Engineer's Guide to Digital Signal Processing*. California Technical Publishing, San Diego, CA, USA, 640 pp.
- Stull, R.B., 1988. *An Introduction to Boundary Layer Meteorology*. Kluwer Academic Publishers, Dordrecht, 666 pp.
- Tuzson, B., Mohn, J., Zeeman, M.J., Werner, R.A., Eugster, W., Zahniser, M.S., Nelson, D.D., McManus, J.B., Emmenegger, L., 2008. High precision and continuous field measurements of δ¹³C and δ¹⁸O in carbon dioxide with a cryogen-free QCLAS. *Appl. Phys. B* 92, 451–458.

- Verma, S.B., Ullman, F.G., Billesbach, D., Clement, R.J., Kim, J., Verry, E.S., 1992. Eddy correlation measurements of methane flux in a northern peatland ecosystem. *Boundary-Layer Meteorol.* 58, 289–305.
- Vickers, D., Mahr, L., 1997. Quality control and flux sampling problems for tower and aircraft data. *J. Atmos. Ocean. Technol.* 14, 512–526.
- Vickers, D., Thomas, C., Law, B.E., 2009. Random and systematic CO₂ flux sampling errors for tower measurements over forests in the convective boundary layer. *Agric. For. Meteorol.* 149, 73–83.
- von Neumann, J., Kent, R.H., Bellinson, H.R., Hart, B.I., 1942. The mean square successive difference. *Ann. Math. Stat.* 12, 153–162.
- Werle, P., Mücke, R., Slemr, F., 1993. The limits of signal averaging in atmospheric trace gas monitoring by tunable diode laser absorption spectroscopy. *Appl. Phys. B* 57, 131–139.
- Werle, P., 1996. Tunable diode laser absorption spectroscopy: recent findings and novel approaches. *Infrared Phys. Technol.* 37, 59–66.
- Werle, P., 1998. A review of recent advances in laser based gas monitors. *Spectrochim. Acta A* 54, 197–236.
- Werle, P., Kormann, R., 2001. A fast chemical sensor for eddy correlation measurements of methane emissions from rice paddy fields. *Appl. Opt.* 40, 846–858.
- Werle, P., Mazzinghi, P., D'Amato, F., De Rosa, M., Maurer, K., Slemr, F., 2004. Signal processing and calibration procedures for in-situ diode laser absorption spectroscopy. *Spectrochim. Acta A* 60, 1685–1705.
- Werle, P., D'Amato, F. (Eds.), 2008. Field laser applications in industry and research. *Appl. Phys. B* 92, 303–467 (special issue).
- Werle, P., D'Amato, F., Viciani, S., 2008. Tunable diode-laser spectroscopy: principles, performance, perspectives. In: Lackner, M. (Ed.), *Lasers in Chemistry—Probing Matter*. Wiley-VCH, Weinheim, pp. 255–275.
- Wienhold, F.G., Frahm, H., Harris, G.W., 1994. Measurements of N₂O fluxes from fertilized grassland using a fast response tunable diode laser spectrometer. *J. Geophys. Res.* 99, 16557–16568.
- Zahniser, M.S., Nelson, D.D., McManus, J.B., Keibian, P.L., 1995. Measurement of trace gas fluxes using tunable diode laser spectroscopy. *Philos. Trans. R. Soc. Lond. Ser. A* 351, 371–382.